

# Surface Structure Determinations with Ion Beams

NICHOLAS WINOGRAD\* and BARBARA J. GARRISON

Department of Chemistry, The Pennsylvania State University, University Park, Pennsylvania 16802

Received March 4, 1980

During the last decade, the research objectives of most surface chemists have turned from an interest in macroscopic aspects of interfacial chemical reactions to the development of atomic descriptions of the surface chemical bond. This more advanced understanding now seems feasible, since many spectroscopic methods have entered the scene that can provide the same type of information which has been available on bulk phase systems since the 1930s. Most of the present effort is directed at determining either atomic positions of atoms or small molecules adsorbed on metal single-crystal surfaces or the detailed nature of the molecular orbitals which participate in the bond.

The question of atomic structure seems most crucial since correct nuclear coordinates facilitate electronic structure calculations. The battery of techniques presently available may well be adequate to solve the structure problem, although uncertainties in how to interpret the spectroscopic results have restricted most work to fairly simple, model-type systems. For example, the location of a sulfur atom on a Ni(001) surface has just recently been determined to be 1.3 Å above the surface Ni plane and presumably in a fourfold coordination site. The same value has been obtained using low-energy electron diffraction (LEED),<sup>1</sup> photoelectron diffraction (PhD),<sup>2</sup> and other photoemission techniques.<sup>3</sup> The bond distance is not found to be much different than that obtained for bulk NiS. A few other isolated surface bond distances have been determined using a surface EXAFS method<sup>4a</sup> and an ion back-scattering technique.<sup>4b</sup> As far as we know, however, the NiS case is the only example where the same result has been obtained by three different methods. And, although many LEED structure determinations have been published,<sup>5</sup> in the absence of supporting data from other methods the reliability of the results is still usually open to discussion.

## Ion Bombardment Methods

Here we wish to focus on the question of the atomic structure of surfaces utilizing ion beams of sufficient

energy to induce nuclear rearrangements which are controlled by the original configuration of atoms. With this approach, the incident ion, usually an inert gas such as He<sup>+</sup>, Ne<sup>+</sup>, or Ar<sup>+</sup>, is accelerated to a kinetic energy of 200–5000 eV and focused onto the sample surface. The momentum exchange between the primary ion and the atoms of the lattice is sufficient to initiate some atomic motion which has a component of momentum moving out into the vacuum. If this component is sufficient to overcome the surface binding forces, then some secondary particles may be found to eject from the solid.<sup>6</sup> A fraction of these particles are ionized as they leave the surface and can, therefore, be detected directly with a mass spectrometer (i.e., as in secondary ion mass spectrometry or SIMS). The SIMS technique has been of considerable recent interest to the surface analyst, since for elements with low ionization potentials or high electron affinities (e.g., H<sup>+</sup>, Na<sup>+</sup>, K<sup>+</sup>, O<sup>-</sup>, Cl<sup>-</sup>, Br<sup>-</sup>, F<sup>-</sup>) the limit of detection can approach 10<sup>-14</sup> g.<sup>7</sup> Furthermore, the primary ion can be focused to a diameter of 100 nm, allowing high spatial resolution. The ion microprobe has found numerous applications in the fields of geology, biology, semiconductor technology, and metallurgy.<sup>8</sup> It is also possible, although generally with a large loss in sensitivity, to utilize some sort of post-ionization of the neutral species.<sup>9</sup> This approach eliminates the large variations of the ion yield with the surface electronic properties, making the technique more quantitative.

To utilize SIMS for examination of surface structure, at least two major problems have to be solved. First, the primary ion beam is known to induce a great deal of damage which can alter the chemical nature of the sample. In 1970, Benninghoven proposed that if the total primary dose (the number of ions/cm<sup>2</sup> to strike

(1) M. Van Hove and S. Y. Tong, *J. Vac. Sci. Technol.*, **12**, 230 (1975); S. Anderson, J. B. Pendry, B. Kasemo, and M. Van Hove, *Phys. Rev. Lett.*, **31**, 595 (1973).

(2) S. D. Kevan, D. H. Rosenblatt, D. R. Denley, B.-C. Lu, and D. A. Shirley, *Phys. Rev. B*, **20**, 4133 (1979).

(3) C. H. Li and S. Y. Tong, *Phys. Rev. Lett.*, **40**, 46 (1978).

(4) (a) P. H. Citrin, P. Eisenberger, and R. C. Hewitt, *Surf. Sci.*, **89**, 28 (1979). (b) J. F. Van Der Veen, R. M. Tromp, R. G. Smeenk, and F. W. Saris, *Surf. Sci.*, **82**, 468 (1979).

(5) M. A. Van Hove, *Surf. Sci.*, **81**, 1 (1979).

(6) This phenomenon is often referred to as sputtering. Since the dictionary definition of sputter is "To emit saliva from the mouth in small particles . . .", we have, in general, avoided this type of jargon.

(7) A. Benninghoven, *Surf. Sci.*, **28**, 541 (1971).

(8) An excellent illustration of the general applicability of SIMS is given by the papers of an international meeting held in Palo Alto, CA, Aug 27–31, 1979, and published in *Springer Ser. Chem. Phys.*, **9** (1979).

(9) H. Oechsner, W. Ruhe, and E. Stumpe, *Surf. Sci.*, **85**, 289 (1979).

Nicholas Winograd was born in New London, CN, in 1945. He received his Ph.D. in Chemistry from Case Western Reserve University in 1970 and immediately joined the faculty of Purdue University. He moved to The Pennsylvania State University in 1979 as Professor of Chemistry. Winograd has been an Alfred P. Sloan Fellow and a John Simon Guggenheim Fellow.

Barbara J. Garrison was born in Big Rapids, MI. After she obtained her Ph.D. from the University of California at Berkeley in 1975, she did postdoctoral work at Purdue and held a lectureship at Berkeley. She joined the faculty at The Pennsylvania State University as an Assistant Professor in 1979. She has won a Camille and Henry Dreyfus Award for newly appointed faculty and has been named an Alfred P. Sloan Fellow for 1980.

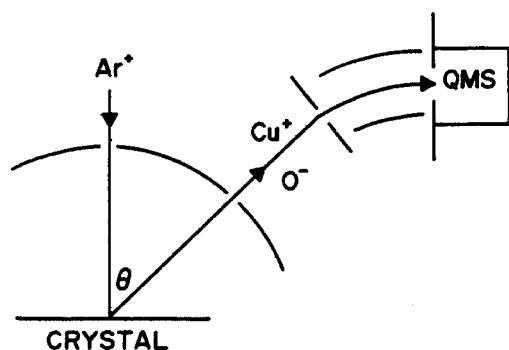


Figure 1. Schematic representation of the SIMS experiment.

the sample during the entire measurement) was kept at least an order of magnitude below the number of surface molecules that these spurious effects could be sufficiently minimized.<sup>10</sup> In practice, this plan amounts to exposing the sample to a  $10^{-9}$ -A beam over a large area of  $\sim 1$  cm<sup>2</sup> for about  $10^2$ – $10^3$  s. This "static" approach is still sensitive enough to detect small fractions of a monolayer, and the spectra can then be interpreted in terms of the original surface structure. The experimental configuration for this setup is illustrated in Figure 1. Using a similar experimental scheme, several research groups have examined a number of model systems including CO, O<sub>2</sub>, and H<sub>2</sub> on Ni,<sup>11–13</sup> O<sub>2</sub> and CO on Mo,<sup>14,15</sup> and O<sub>2</sub> on W,<sup>16</sup> to name just a few. The resulting ion yields certainly reflect the coverage and chemical state of the adsorbate. For example, molecularly adsorbed CO can be distinguished from dissociatively adsorbed CO from the NiCO<sup>+</sup> cluster ion yield, although any kind of "first principles" understanding of the spectra is still missing.

### Classical Dynamics Calculations

This interpretation problem brings us to the second major stumbling block in applying SIMS to the characterization of surface structure, which is that no atomistic description of the ion bombardment process presently exists. To provide some insight into solving this problem, we have been utilizing a classical dynamics procedure to compute the positions and momenta of all the relevant particles as a function of time after impact of the primary ion. This approach has, of course, been very successful in examining trajectories in atom-diatom scattering,<sup>17</sup> properties of liquids,<sup>18</sup> and even the solvation of large molecules like dipeptides.<sup>19</sup> For our case, the infinite solid can be approximated by a microcrystallite which is, generally, four atomic layers deep containing about 60 atoms/layer.<sup>20</sup> From the

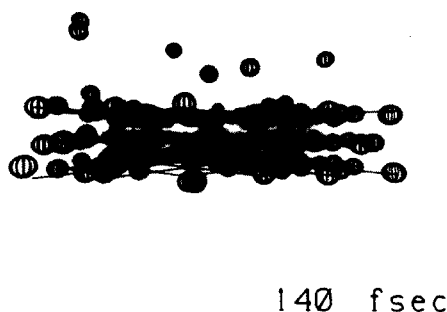
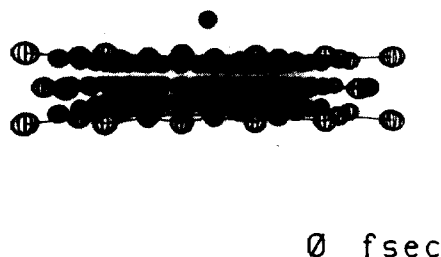


Figure 2. Positions of the atoms. (a) Before the primary ion (the lone sphere above the solid) has struck. (b) Consequences of a single ion impact. The two atoms ejecting to the left form a dimer. For graphical clarity, only a selected group of atoms is shown, and their size is arbitrarily drawn for best graphical clarity.

results of the calculations for a Ni(001) crystal, it is clear that the consequences of a single ion impact are quite dramatic, as illustrated in Figure 2. Nearly all of the atoms are observed to be perturbed from their initial positions. Some of the atoms found above the surface will indeed eject into the vacuum. Other slow-moving particles can be pulled back to the solid by attractive interactions.

In practice, somewhere between 100 and 1000 trajectories are computed at impact points over an irreducible surface symmetry zone to obtain the macroscopic yield of particles and other observables. The calculation during a single ion trajectory is stopped after it is energetically impossible for the fastest moving atom to eject. The size of the model microcrystallite is ideally selected such that further size increases do not change the observable of interest. The model is quite general in that different crystal structures or faces can be set up. Chemisorbed atoms or molecules can be placed in arbitrary locations and coverages on the microcrystallite surface. The details of the procedure can be found in several of our early papers.<sup>20–22</sup>

Although the classical dynamics procedure is an extremely powerful one which is ideally suited to describing such a complex process, there are two difficulties that prevent a complete solution to the problem. First, in order to calculate the forces between atoms, one generally must know the interaction potential surface for all the atoms in the microcrystallite. There has been a lot of effort expended to attempt to find the

(10) A. Benninghoven, *Z. Phys.*, **230**, 403 (1970); *Surf. Sci.*, **53**, 596 (1975).

(11) K.-H. Mueller, P. Beckmann, M. Schemmer, and A. Benninghoven, *Surf. Sci.*, **80**, 325 (1979).

(12) R. S. Bardoli, J. C. Vickerman, and J. Wolstenholme, *Surf. Sci.*, **85**, 244 (1979).

(13) T. Fleisch, G. L. Ott, W. N. Delgass, and N. Winograd, *Surf. Sci.*, **81**, 1 (1979).

(14) P. H. Dawson, *Surf. Sci.*, **71**, 247 (1978).

(15) P. H. Dawson, *Phys. Rev. B*, **15**, 5522 (1977).

(16) M. L. Yu, *Surf. Sci.*, **71**, 121 (1978).

(17) See, for example, D. G. Truhlar and J. T. Muckerman in "Atom Molecule Collision Theory", R. B. Bernstein, Ed., Plenum Press, New York, 1979.

(18) See, for example, P. Lykos, Ed., *ACS Symp. Ser.*, No. 86 (1978).

(19) D. J. Rossky and M. Karplus, *J. Am. Chem. Soc.*, **101**, 1913 (1979).

(20) D. E. Harrison, Jr., P. W. Kelly, B. J. Garrison, and N. Winograd, *Surf. Sci.*, **76**, 311 (1978).

(21) B. J. Garrison, N. Winograd, and D. E. Harrison, Jr., *Phys. Rev. B*, **18**, 6000 (1978).

(22) B. J. Garrison, N. Winograd, and D. E. Harrison, Jr., *J. Chem. Phys.*, **69**, 1440 (1978).

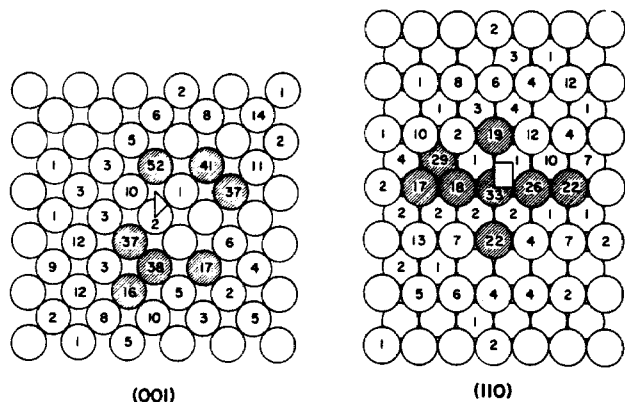


**Figure 3.** Ejection of atoms from the bombardment of copper by 600-eV  $\text{Ar}^+$  ions at normal incidence. (a) Cu(001), (b) Cu(110). The numbers refer to the percentage of ion impacts in which the particular atom was ejected. The shaded atoms are the ones ejected most frequently. The symmetry zone for the ion impacts is shown on each face.

correct potentials, and although certain forms have gained popularity, it is not clear that any are indeed accurate. Our approach has been to construct a pairwise additive function from an exponential repulsion at small internuclear separations and a long-range Morse attractive part.<sup>21,23</sup> We then restrict our calculations to circumstances which are not strongly dependent on the uncertain potential parameters. The relative yields of atoms ejected from different crystal faces of the same metal represent such an example.<sup>24</sup> The second difficulty is that the ionization probability of a given particle is not considered in the calculation, whereas SIMS experiments detect only the ions. It is our hypothesis that the trajectories of the ions are quite similar to those of the neutrals, especially at higher kinetic energies. This is borne out in part by noting that similar angular distributions and energy distributions are measured for both  $\text{Cu}^+$  and  $\text{Cu}^0$  ejected from metallic copper.<sup>25,26</sup> We further note that certain ion yield ratios compare well with the same calculated yield ratio for the neutral species.<sup>27</sup> Despite these difficulties, we believe that this classical dynamics approach has provided the necessary base from which the applications of the ion bombardment techniques can expand.

### Structure-Sensitive Factors

Probably the most striking feature to come out of our early analyses of the detailed particle motion was that the ejection mechanisms and yields were critically dependent on the crystal orientation.<sup>20</sup> In Figure 3, for example, note that from a Cu(001) face the target atom is rarely observed to be emitted since it is generally driven down into the bulk of the crystal. On a (110) face, however, the target atom can reflect from the second layer and easily find an ejection pathway. In

(23) Our procedures essentially follow the pioneering work of D. E. Harrison, Jr., in setting up the basic computational scheme as from D. E. Harrison, Jr., W. L. Moore, Jr., and H. T. Holcombe, *Radiat. Eff.*, **17**, 167 (1973).

(24) N. Winograd, D. E. Harrison, Jr., and B. J. Garrison, *Surf. Sci.*, **78**, 767 (1978).

(25) V. E. Yurasova, A. A. Sysoev, G. A. Samsonov, V. M. Bukhanov, L. N. Nevzorova, and L. B. Shelyakin, *Radiat. Eff.*, **20**, 89 (1973).

(26) S. P. Holland, B. J. Garrison, and N. Winograd, *Phys. Rev. Lett.*, **43**, 220 (1979).

(27) H. Oechsner and W. Gerhard, *Surf. Sci.*, **44**, 480 (1974).

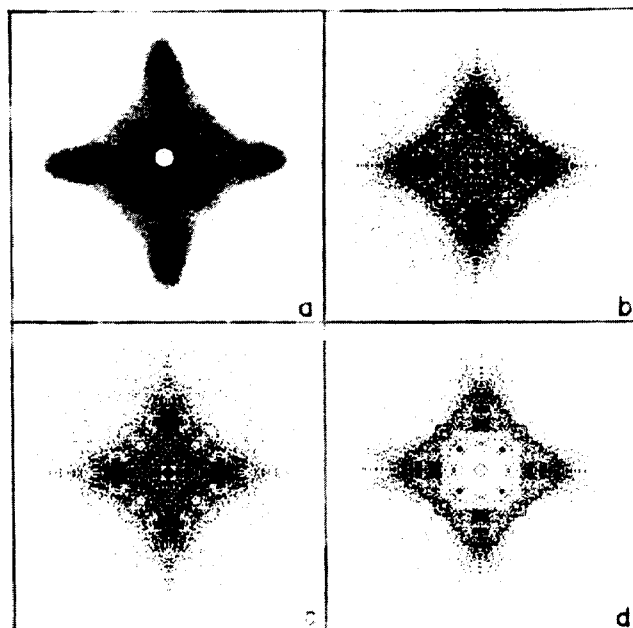


**Figure 4.** Angular distribution of particles ejected due to  $\text{Ar}^+$  ion bombardment at normal incidence of an (001) face of an fcc metal. (a) Experimental result taken for 4-keV  $\text{Ar}^+$  ions bombarding Cu (A. L. Southern, W. R. Willis, and M. T. Robinson, *J. Appl. Phys.*, **34**, 153 (1963)). (b) Calculated result for 1-keV  $\text{Ar}^+$  ions bombarding Ni (particles of all kinetic energies are shown). (c) Only those particles whose kinetic energy is less than 10 eV are shown. (d) Only those particles whose kinetic energy is greater than 10 eV are shown.

fact, it is this particle which ejects most frequently.

A second aspect of this concept comes from an analysis of the angular distributions of the secondary particles. In the late 1960s, Wehner noted that by placing a flat plate collector an arbitrary distance above the crystal the Cu atoms formed a pattern which reflected the symmetry of the crystal surface.<sup>28</sup> Many other laboratories investigated this phenomenon, resulting in over 100 publications. Interest in the area waned in the early 1970s, however, since vacuum conditions were less than ideal and no theory evolved which quantitatively explained the results. The experiment was further clouded by the use of very high primary ion doses where the surface crystal structure could clearly be perturbed.

Two questions come out of the early realizations that the crystal structure dominates the mechanism of particle ejection. First, why should it be so at all? From Figure 2, it is clear that the crystal order is grossly altered during a trajectory, converted into nearly a liquid-like state. Should not the preferred ejection channels in the crystal be destroyed by the ion beam itself? Secondly, if the crystal effects are observed, can they be extended to include adsorbate atoms where the angular distributions of those species would reflect their location on the surface?

The genesis of Wehner's spots and the question about the adsorbate geometry can be readily probed with the classical dynamics calculations and the results can be used to predict some fascinating new experiments. As can be seen in Figure 4a,b, the features of the calculations are quite close to the early measured spot pat-

(28) For a good review of this topic, see G. Carter and J. S. Colligan, "Ion Bombardment of Solids", American Elsevier, New York, 1968.

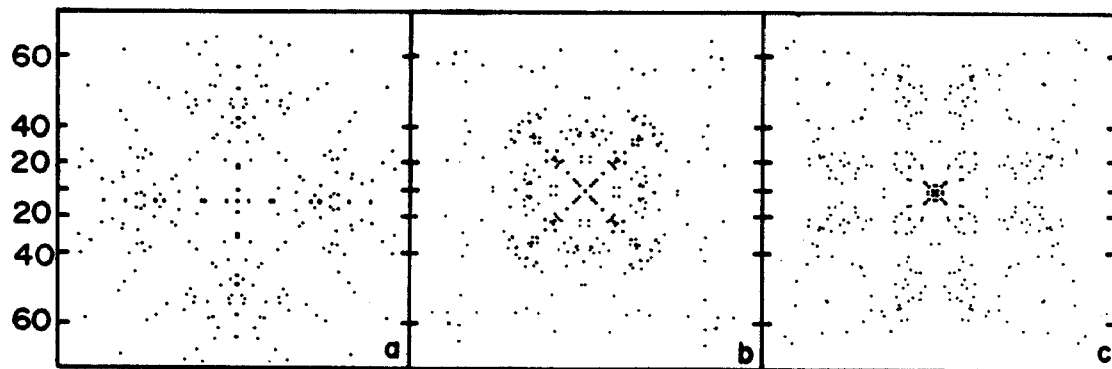


**Figure 5.** Calculated angular distributions of oxygen atoms ejected due to  $\text{Ar}^+$  ion bombardment at 600 eV. The oxygen originated in a  $c(2 \times 2)$  coverage on  $\text{Cu}(001)$  in various site symmetries and heights above the surface,  $h$ . The numbers refer to the polar deflection angle. (a) A-top or linearly bonded site,  $h = 1.9 \text{ \AA}$ . (b) Fourfold bridge site,  $h = 1.2 \text{ \AA}$ . (c) Fourfold bridge site,  $h = 0.9 \text{ \AA}$ .

terns,<sup>29</sup> giving us considerable confidence in applying the model to some untried experimental conditions. To discern the exact cause of the strong anisotropy, we must turn to a consideration of the energy distribution of the secondary particles. Although these curves have been discussed in detail,<sup>30</sup> here we emphasize only that the distribution begins at zero at 0.0 eV, rises to a maximum at an energy between 1 and 5 eV, and falls off as  $\sim E^{-1.6}$ . There is a significant fraction of particles which leave the solid with a kinetic energy greater than 10 eV, perhaps 20–40%. Since these particles eject early in the collision sequence before a great deal of the crystallography is interrupted, we believed that these higher energy particles might be responsible for the observed strong anisotropy. In Figure 4d, then, we display these patterns for the (001) surface after removing all particles whose kinetic energy is less than 10 eV. Note that the rather diffuse background clearly evident in Figure 4b,c has been filtered out, leaving only the strongly directed particles. As it turns out, this energy selection process also simplified dramatically the number of operative ejection mechanisms, as the spot is composed nearly entirely from the atoms near the target atom which eject frequently (labeled 38, 41, 52, and 37 (2) in Figure 3a). Since these particles are found to originate near the target atom, long-range surface order should not be required to produce the spot. A further consequence of examining only the higher energy particles is that the trajectory can be stopped after a shorter number of time steps and accurate trajectories can be obtained by using much smaller microcrystallites.

The answer to the first question is then clear. The spots are produced by the fast-moving particles since they can be channeled by a small part of the surface while it is still intact. To examine the second question, we derived a computational scheme to place a model adsorbate atom with the mass of oxygen on the  $\text{Cu}(001)$  surface.<sup>21</sup> We estimated the interaction potential between oxygen and the copper by scaling the Cu–Cu interaction and by selecting other parameters appropriate for the  $\text{CuO}$  molecule. The geometry and coverage of the adsorbate could be varied over a wide range to test how these quantities influenced the angular distributions. The result was quite spectacular, espe-

cially for the higher energy oxygen atoms. In Figure 5a,b, for example, we show the relevant distributions for oxygen placed in an A-top adsorption site and in a fourfold bridged coordination site.<sup>29</sup> Note that the distributions of the substrate copper atoms maintain their basic symmetry, although the shape of the spot is altered slightly. For the adsorbate, the A-top configuration exhibits ejection angles with mainly the same symmetry as the substrate. For the bridged configuration, however, the pattern is rotated by  $45^\circ$  with respect to the substrate and is easily distinguishable from the other geometry.

The scattering mechanisms that give rise to these patterns can be discerned on an atomic level from an analysis of the trajectories. It is sufficient to note here that the ejecting substrate atoms most strongly influence the directions of the ejecting adsorbate atoms and that multiple scattering in the overlayer is of secondary importance. This result portends that the angular distributions of the oxygen atom might even be sensitive to its height above the surface when placed in a given geometry. This hypothesis is borne out in Figure 5c where the oxygen height is reduced from 1.2  $\text{\AA}$  to 0.9  $\text{\AA}$  above the Cu plane. The theory suggests that with sufficiently accurate measurements atomic positions should be determinable to better than  $\pm 0.1 \text{ \AA}$ .

Experimental verification of these predictions has been carried out to a limited extent.<sup>26</sup> To measure the angular distributions of ejected oxygen and copper atoms, a cylindrical shield was placed above the crystal surface as shown in Figure 1. The polar angle,  $\theta$ , for ejected species was fixed at  $45^\circ$  with two appropriately placed apertures while the azimuthal angle,  $\phi$ , could be varied over  $360^\circ$  by rotation of the crystal. When the  $45^\circ$  electrostatic sector in front of the mass spectrometer was utilized, the kinetic energies of the ejected particles could be roughly selected while a large enough bandpass necessary to maintain sensitivity was still kept. This experimental configuration will produce results equivalent to making a circular cut of the spot pattern at a radius corresponding to the  $45^\circ$  polar deflection but does not allow the entire pattern to be reproduced. It is possible to prepare a  $c(2 \times 2)$  overlayer of oxygen on  $\text{Cu}(001)$  by exposure of the crystal to 1200 L (1 L =  $10^{-6}$  torr s) of  $\text{O}_2$  at  $25^\circ \text{C}$ .

The observed azimuthal plots for  $\text{Cu}^+$  and  $\text{O}^-$  ejection from these samples are shown in Figure 6a. The fourfold symmetry of the (001) orientation is clearly evident for both species, although their maxima in in-

(29) N. Winograd, B. J. Garrison, and D. E. Harrison, Jr., *Phys. Rev. Lett.*, **41**, 1120 (1978).

(30) B. J. Garrison, N. Winograd, and D. E. Harrison, Jr., *Surf. Sci.*, **87**, 101 (1979).

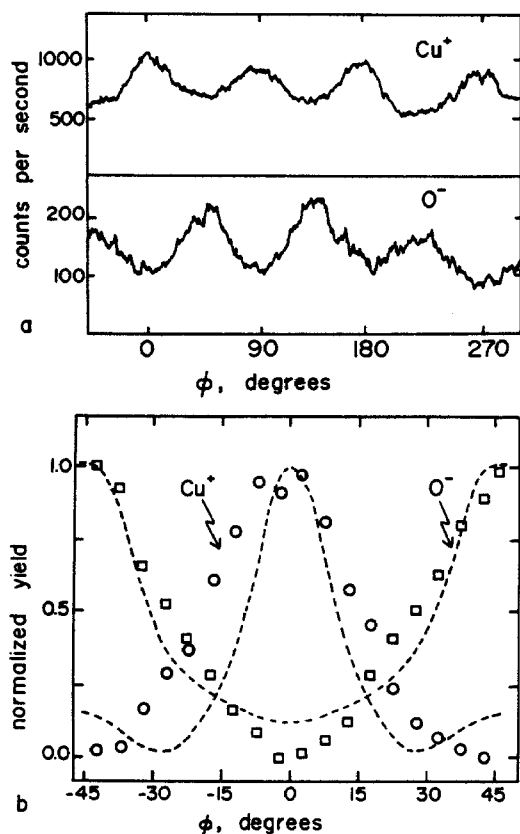


**Figure 6.** Azimuthal angular distributions. (a) The  $\text{Cu}^+$  and  $\text{O}^-$  azimuthal plots recorded from the spectrometer. The primary ion is 1500-eV  $\text{Ar}^+$  at a total dose of  $10^{13}$  ions/ $\text{cm}^2$ . (b) A fourfold average of the data in (a) with the minimum intensity subtracted from each curve. The dashed lines represent the calculated curve for O placed in a fourfold bridge site 1.2 Å above the Cu plane. The circles represent the  $\text{Cu}^+$  intensities and the squares the  $\text{O}^-$  intensity.

tensity are out of phase by  $45^\circ$ . This result is only consistent with the calculated results if the oxygen has adsorbed in the fourfold bridge site. The detailed comparison taken using a fourfold averaging and background subtraction procedure is shown in Figure 6b, assuming the oxygen is 1.2 Å above the surface. If the calculation had been performed for oxygen placed only 0.9 Å above the surface, the predicted curve would be considerably different.<sup>26</sup>

### Cluster Formation Processes

By taking advantage of the ejection directions of atoms from chemically reacted surfaces, it seems feasible, then, to obtain adsorption-site information quite simply. A second aspect of the ion bombardment process involves the fact that molecular cluster species are often observed to be ejected from the surface. For adsorbates on clean metals, these vary from pure metal clusters  $\text{M}_n$ , where  $n$  can be as large as 12 or more<sup>31</sup> to metal atoms attached to adsorbed species, e.g.,  $\text{NiO}$  or  $\text{NiCO}$ ,<sup>13,32</sup> to large organic molecules that were originally adsorbed on the surface of the solid which eject retaining their molecular formula.<sup>33,34</sup> Some examples

(31) G. Staudenmaier, *Radiat. Eff.*, **13**, 87 (1972).

(32) T. Fleisch, W. N. Delgass, and N. Winograd, *Surf. Sci.*, **78**, 141 (1978).

(33) H. Grade, R. G. Cooks, and N. Winograd, *J. Am. Chem. Soc.*, **99**, 7725 (1977).

(34) A. Benninghoven and W. K. Sichtermann, *Anal. Chem.*, **50**, 1180 (1978).

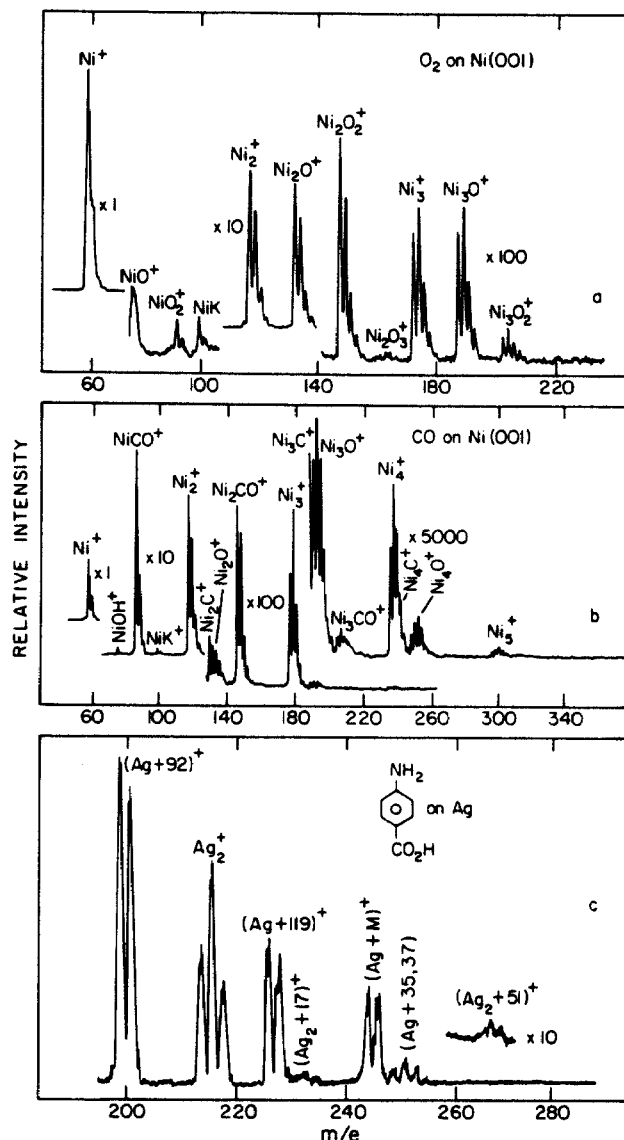


**Figure 7.** Experimental SIMS spectra. (a) Positive ion spectrum for Ni(001) exposed to 30 L of oxygen. (b) Positive ion spectrum for Ni(001) exposed to 2 L of CO. (c) Positive ion spectrum for p-aminobenzoic acid adsorbed on polycrystalline Ag.

of these spectra are shown in Figure 7.

It has been intriguing to speculate about the origin of these clusters. If they arise from contiguous surface atoms, then their presence could provide key information regarding the local atomic structure of complex surfaces such as alloys and supported metal catalysts. They may also yield information regarding surface bonding geometries. The  $\text{Ni}_2\text{CO}^+$  cluster, for example, has been proposed to originate from a bridge-bonded CO complex on Ni, while the  $\text{NiCO}^+$  cluster has been associated with a singly or linearly bonded Ni-CO complex.<sup>12</sup>

From the classical dynamics treatment, it is possible to examine the cluster formation mechanism in detail and to provide semiquantitative information about cluster yields. In general, these calculations tell us that there are three basic mechanisms of cluster formation.<sup>35</sup> First, for clean metals or metals covered with atomic adsorbates, the ejected atoms can interact with each

(35) B. J. Garrison, N. Winograd, and D. E. Harrison, Jr., *J. Vac. Sci. Technol.*, **16**, 789 (1974).

other in the near surface region above the crystal to form a cluster via a recombination type of process.<sup>21,22,24</sup> This description would apply to clusters of metal atoms and of metal-oxygen clusters of the type  $M_nO_m$  observed in many types of SIMS experiments and illustrated in Figure 7a. For this case the atoms in the cluster do not need to arise from contiguous sites on the surface, although we do find that in the absence of long-range ionic forces most of them originate from a circular region of radius  $\sim 5$  Å. This rearrangement, however, complicates any straightforward deduction of the surface structure from the composition of the observed clusters. A second type of cluster emission involves molecular adsorbates like CO adsorbed onto Ni as shown in Figure 7b. Here, the CO bond strength is  $\sim 11$  eV, but the interaction with the surface is only about 1.3 eV. Our calculations tell us<sup>36</sup> that this energy difference is sufficient to allow CO to eject molecularly, although we do find that  $\sim 15\%$  of them can be dissociated by the ion beam or by energetic metal atoms. Clearly, for the case of these molecular systems, it is easy to infer the original atomic configurations of the molecule and to determine the surface chemical state. If CO were dissociated into oxygen and carbon atoms, for example, our calculations suggest that the amount of CO observed should drop dramatically. This type of process undoubtedly applies to the adsorption of organic molecules on surfaces, since the strong carbon framework can soak up excess energy from violent collisions.<sup>37</sup> The final mechanism for cluster ejection is essentially a hybrid mechanism between the first two. For the case of CO on Ni again, we find that the observed NiCO and Ni<sub>2</sub>CO clusters form by a recombination of ejecting Ni atoms with ejecting CO molecules. There is apparently no direct relationship between these moieties and linear and bridge-bond surface states. A similar mechanism ought to apply to the formation of cationized organic species shown in Figure 7c. The organic molecule ejects intact, but interacts with an ejecting metal ion to form a new cluster species.<sup>37</sup>

The fact that the composition of the ejected clusters may vary from the original arrangement of surface atoms is somewhat discouraging. As it turns out, however, there are possible situations where the precise nature of the rearrangement can be predicted theoretically. One example involves the measured  $O_2^-/O^-$  ratio as a function of oxygen coverage on Ni(001). This ratio is four times higher for the 50% oxygen coverage [ $c(2 \times 2)$ ] than for the 25% oxygen coverage [ $p(2 \times 2)$ ], a change which is also calculated with the model.<sup>38</sup> The reason for this effect is that there are no closely neighboring oxygen atoms on the  $p(2 \times 2)$  surface, and the  $O_2$  formation probability is much lower. Employing concepts of this sort may be useful in testing for island-growth mechanisms and distinguishing them from those which proceed through several distinct phases.

Another important concept relative to the rearrangement problem involves the selection of the angle of incidence of the primary particle as well as the energy and angle of the ejected species in order to tune in to

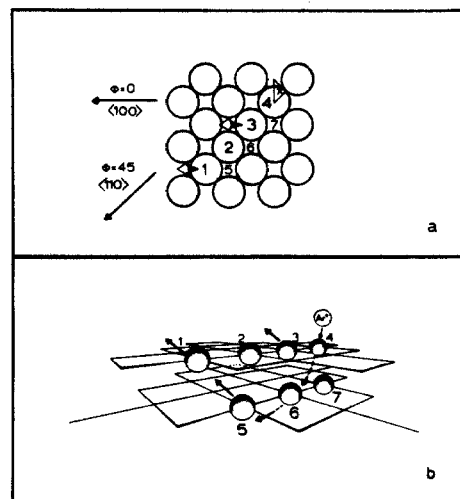


**Figure 8.** Mechanism of formation of the Ni<sub>2</sub> dimer which preferentially ejects in the  $\langle 100 \rangle$  directions, contributing the majority of intensity to the peak in the angular distribution. (a) Ni(001) showing the surface arrangements of atoms. The numbers are labels while the  $\times$  denotes the Ar<sup>+</sup> ion impact point for the mechanism shown in Figure 8b. Atoms 1 and 3 eject as indicated by the arrows forming a dimer, which is preferentially moving in a  $\langle 100 \rangle$  direction. (b) Three-dimensional representation of a Ni<sub>2</sub> dimer formation process. The thin grid lines are drawn between the nearest-neighbor Ni atoms in a given layer. For graphical clarity, only the atoms directly involved in the mechanism are shown.

specific ejection pathways. On Ni(001), for example, there is considerable azimuthal anisotropy of the dimer Ni<sub>2</sub><sup>+</sup> as well as the monomer Ni<sup>+</sup>. For the higher energy dimers, the calculations predict that at  $\phi = 0^\circ$  nearly all are formed from the specific mechanism illustrated in Figure 8. With this process, then, the observed dimers should originate from next-nearest neighbors along the close-packed row.<sup>39</sup> In a similar vein, calculations examining oblique angles of incidence of the primary Ar<sup>+</sup> ion have shown that other mechanisms of dimer formation and, hence, other originating sites can be preferentially enhanced.<sup>40</sup>

## Prospects

The combinations of the ion bombardment experiments on well-defined single crystals and the results of theoretical classical dynamics calculations have provided a sound basis from which to proceed with the goal of characterizing surface structure. The analysis of the angular distributions of both the ejected atoms and clusters indicates that unique geometrical information about the configuration of surface atoms can be obtained. The approach should prove to be an excellent complement to LEED—a tool which is very sensitive to the choice of scattering potential and very insensitive to the adsorbate registry—and to angle-resolved photoemission which has proved useful in elucidating molecular geometries on surfaces.<sup>2</sup> On the other hand, the computation of accurate absolute yields must await the availability of better interaction potential functions. The model also provides a good starting point in which to interpret SIMS spectra. Currently, the ionization phenomena is the lacking piece of the theory, but by taking ratios of ion yields, semiquantitative comparisons

(36) B. J. Garrison, N. Winograd, and D. E. Harrison, Jr., *J. Chem. Phys.*, in press.

(37) B. J. Garrison, *J. Am. Chem. Soc.*, in press.

(38) N. Winograd, B. J. Garrison, T. Fleisch, W. N. Delgass, and D. E. Harrison, Jr., *J. Vac. Sci. Technol.*, 16, 629 (1979).

(39) S. P. Holland, B. J. Garrison, and N. Winograd, *Phys. Rev. Lett.*, 44, 756 (1980).

(40) K. E. Foley and B. J. Garrison, *J. Chem. Phys.*, 72, 1018 (1980).

can be made. In addition, the fact that atomic trajectories can be followed on a microscopic level is an advantageous feature in coupling ionization theories which will necessarily include the kinetic energy of the particle and its temporal local atomic environment.

*We are particularly grateful to Don Harrison for willingly providing us with a working computer program and for all his direct efforts in teaching us his unique insight into the ion bombardment process. The interaction with an exceptional group of collaborators has made possible the development of these ideas. These people include Professors Don Harrison, Nick*

*Delgass, and Graham Cooks, Dr. Theo Fleisch, and graduate students Steven Holland, Richard Gibbs, and Karin Foley. The financial support of the National Science Foundation (CHE-79-19605), the Air Force Office of Scientific Research (AFOSR-80-0002), and the donors of the Petroleum Research Foundation administered by the American Chemical Society, are gratefully appreciated. Portions of the computations were supported by the National Resource for Computation in Chemistry under a grant from the National Science Foundation and the U.S. Department of Energy (Contract No. W-7405-ENG-48). B.G. also thanks the Research Corporation, the A. P. Sloan Foundation, and the Dreyfus Foundation for financial support.*